AIAA 81-4213

Probability of Collisions in the Geostationary Ring

Martin Hechler* and Jozef C. Van der Ha†
European Space Operations Centre, ESA, Darmstadt, FRG

Geostationary satellites not removed from the geosynchronous altitude at the end of their useful life will expose future spacecraft orbiting in this unique region to a continual collision hazard. The probability of a collision occurring before the end of this century is less than 2×10^{-3}, unless large space structures such as solar-power satellites become operational, in which case collisions would likely occur every few years. Fundamental data on the collision probabilities are derived from deterministic orbit propagation for a representative sample of uncontrolled objects using an intersection process in which the active satellites are described by a probability distribution within the geostationary ring. The study clearly points out that all geostationary satellites should be removed from the ring at the end of their operational lifetime in order that the collisional risk remains within acceptable bounds in the future. The cost of this remedy amounts to no more than that of one month of active station-keeping for present-day satellites.

Nomenclature

A_c = collisional cross-section area
a = semimajor axis
$\boldsymbol{a}$ = vector of nonsingular orbital elements
e = eccentricity
f,g = components of eccentricity vector, Eq. (3)
$f(x)$ = spatial density of operational satellites along path x in the geostationary ring
h,k = components of polar vector, Eq. (3)
I = collision probability for one pass through the geostationary ring
i = inclination
M = mean anomaly
N_P = Perek number
R = disturbing function
r = radial Earth-satellite distance
r_s = reference geostationary altitude, 42164.2 km
$\bar{v}_{\rm rel}$ = mean relative velocity between operational and deactivated satellites
λ = collision rate per year
Λ = mean longitude, $M+\omega+\Omega$
ρ = relative radial distance $(r-r_s)/r_s$
σ = normalized semimajor axis deviation
ϕ = latitudinal angle, Fig. 1
ω = argument of perigee
ω_E = Earth's rotation rate
Λ = mean longitude, $M+\omega+\Omega$
Ω = longitude of ascending node

Introduction

THE number of geostationary satellites is currently growing at a rate of about 20 per year, and it is generally expected that in the near future the sizes of geostationary satellites will increase dramatically as antenna platforms and perhaps even huge solar-power satellites beome operational. Obviously, the probability of a collision will grow along with the number and average size of the objects in orbit. It will surpass the level of acceptability sometime in the future due to the accumulation of abandoned satellites orbiting in the same spatial region as the operational spacecraft.

The orbital characteristics of the operational station-kept geostationary satellites are very different from those of the abandoned spacecraft that have reached the end of their useful lifetime. The former class of satellites is characterized by usually very tight requirements (e.g., ±0.1 deg) in the longitudinal and latitudinal coordinates. They are subjected to frequent station-keeping maneuvering so that a deterministic long-term orbit modeling is impossible. They will therefore be represented as a "cloud" of distributed objects and the region in which they may be encountered with positive probability is denoted as the *geostationary ring,* Fig. 1. Detailed properties of their spatial distribution in this ring can be derived from orbital dynamics and from station-keeping statistics.

On the other hand, the abandoned geostationary satellites move freely under the prevailing natural forces and undergo considerable oscillations in latitudinal and, in general, in longitudinal direction in the long run. As there are no long-term secular contributions to their orbital energy, the abandoned satellites should be expected to continue moving permanently through the same spatial region that is occupied by the operational satellites. Because of this long-term predictability, a sample of deterministic orbit evolutions starting from different typical initial conditions for satellites having different typical physical properties can be taken as representative of the motion of the whole population. On the basis of the distinction between active and abandoned geostationary satellites, one may consider the following types of collisions in the geostationary ring: 1) between an operational and an abandoned satellite; 2) between two operational satellites; and 3) between two abandoned satellites.

The first type of collision is undoubtedly the most important one since the growing number of deactivated geostationary satellites will form a perpetual hazard which can not actively be controlled. The second type of collision will become a problem in the future if, because of increasing demand (e.g., from the proposed TV-Sats), the same longitudinal slot has to be shared by more than one satellite. The last type of collision is serious only in so far as it increases the number of uncontrolled objects passing through the geostationary ring, thereby indirectly magnifying the probability of a collision of the first category.

For these reasons, and because the probability of a collision during station acquisition has been found to be negligible, the study has been restricted to two types of collisions: 1) collisions between active and inactive satellites; 2) collisions between active satellites at the same longitude.

In the first case the intersection process of the populations leads to the evaluation of line integrals along the paths of the representative abandoned objects through the geostationary ring. In the second case a multidimensional integral over spatial densities is evaluated by means of a Monte-Carlo

Received Oct. 29, 1980; revision received Feb. 12, 1981. Copyright © American Institute of Aeronautics and Astronautics, Inc., 1980. All rights reserved.

*Mathematical Analyst, Mission Analysis Office.
†Aerospace Engineer, Mission Analysis Office. Member AIAA.

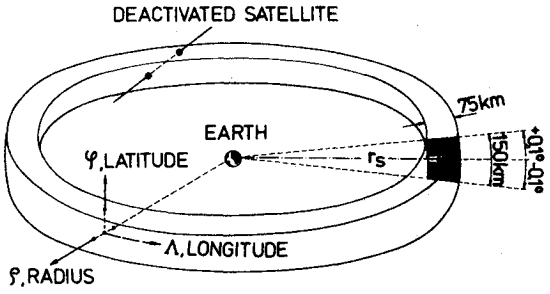

Fig. 1 The 0.1 deg geostationary ring containing operational satellites (not to scale).

method. A detailed account of the present study can be found in two internal reports.[1,2] A summary of the approach taken and the results obtained will be given in this paper. Another independent study on the subject appeared recently.[3]

Summary of Theoretical Approach

Collisional Probabilities

The collision rate[4] for a deterministic object moving through a population of objects, which are described by their spatial distribution, is proportional to the mean effective collisional cross section A_c, the mean relative velocity $\bar{v}_{rel}$, and the spatial density $f(x)$ of the distributed objects along the trajectory $x(t)$:

$$\frac{dI}{dt} = A_c \bar{v}_{rel} \quad f(x) \tag{1}$$

For a path $x(\Lambda)$ followed by an object moving through the geostationary ring, the probability of a collision becomes

$$I = A_c \int_{\Lambda_1}^{\Lambda_2} f(x(\Lambda)) \frac{\bar{v}_{rel}}{\omega_E} d\Lambda \tag{2}$$

Addition of these path integrals over many revolutions of free motion of a deactivated satellite produces the fundamental probabilistic information.

In the case of collisions between active satellites stationed at the same longitude, neither of the objects can be represented deterministically. A rigorous derivation of spatial densities and the relative velocity between the colliding objects, including the correlating effects of dynamics and station-keeping strategies, leads to a nine-dimensional integral which has been evaluated by a Monte-Carlo-type method after some explicit reductions.

Long-Term Orbit Evolution of Abandoned Satellites

The evolution of the orbital elements of a typical sample of deactivated geostationary satellites was determined by numerical integration of an averaged set of perturbation equations. In order to avoid singularities in the rates of change of ω and Ω, the following set of nonsingular equinoctial elements was employed:

$$\left.\begin{aligned} f &= e\cos(\omega+\Omega) \\ g &= e\sin(\omega+\Omega) \end{aligned}\right\} \text{eccentricity vector}$$

$$\left.\begin{aligned} h &= \tan(i/2)\cos\Omega \\ k &= \tan(i/2)\sin\Omega \end{aligned}\right\} \text{polar vector} \tag{3}$$

$$\sigma = (a - r_s)/r_s \qquad \text{normalized semimajor axis deviation}$$

$$\Lambda = M + \omega + \Omega \qquad \text{mean longitude}$$

The variation of these elements under perturbing influences is described by a modified form of the classical Lagrange planetary equations and can be conveniently expressed in terms of the derivatives of a disturbing function R with respect to the elements considered. That is,

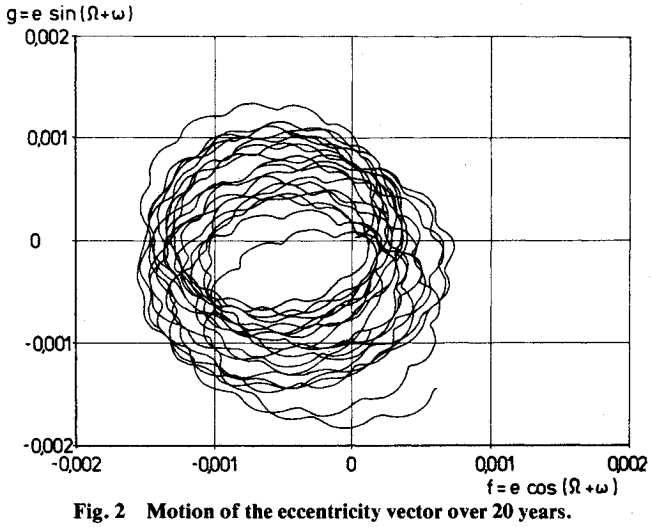

Fig. 2 Motion of the eccentricity vector over 20 years.

$$\dot{a}_j = F_j(a, \partial R/\partial a) \qquad j = 1,\ldots,6 \tag{4}$$

where a_j designates any one of the elements in Eq. (3). The disturbing functions due to each of the following perturbing effects were evaluated: 1) luni-solar perturbations, including the first two parallactic terms for the Moon; 2) Earth's gavitational field perturbations, up to fourth-degree zonal and tesseral harmonics; and 3) solar-radiation-pressure perturbations, and taking a constant reflective area with homogeneous reflectivity properties.

Subsequently, the perturbation equations were averaged analytically over the fast variable Λ—the mean longitude of the satellite. The many tedious calculations involved were performed by automated Poisson series manipulation on a digital computer in order to minimize the occurrence of errors. Extremely compact representations for the secular part of the luni-solar disturbing function could be obtained by recombining the computer-generated results in functions of a few properly chosen parameters. The tesseral resonance effects were captured by expressing the Greenwich hour angle, which is also a fast-varying angle, in terms of the mean longitude before the averaging operation. The ephemerides for the Moon's position and Sun's position were modeled analytically. During the averaging over the satellite's mean longitude, the Sun's position and Moon's position were considered to be slowly varying. The accuracy of the long-term orbit evolution was assessed by comparison of a few test cases with numerical integration of the exact equations over an interval of a few decades.

The results show that the long-term orbit evolution possesses three distinct characteristics with very little cross coupling. These are the eccentricity vector motion, the polar vector motion, and, finally, the semimajor axis vs longitude phase-plane trajectory. For satellites with an area/mass ratio larger than say 0.01 m^2/kg, the eccentricity vector motion (Fig. 2) is principally determined by the solar-radiation-pressure effect which tends to rotate the vector away from the instantaneous Earth-Sun line. Over the period of one year the eccentricity vector describes an almost closed loop, with the curly features caused mainly by the Moon's parallactic term (the figures show the evolution over 20 years).

The polar vector of a geostationary orbit is perturbed mainly by oblateness and luni-solar effects. It precesses with a period of approximately 52 years around a point about 7.3 deg from the equatorial pole in the direction of the pole of the ecliptic (Fig. 3). The nutational ripples in the coning motion have a period of 6 months and are caused by the Sun's gravitational attraction.

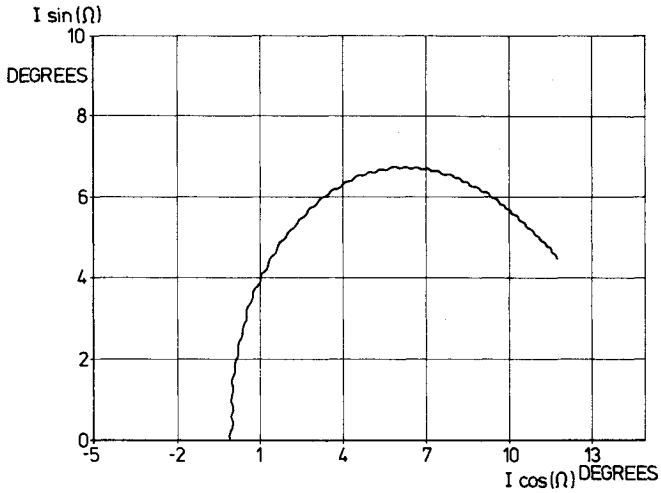

Fig. 3 Motion of the polar vector over 20 years.

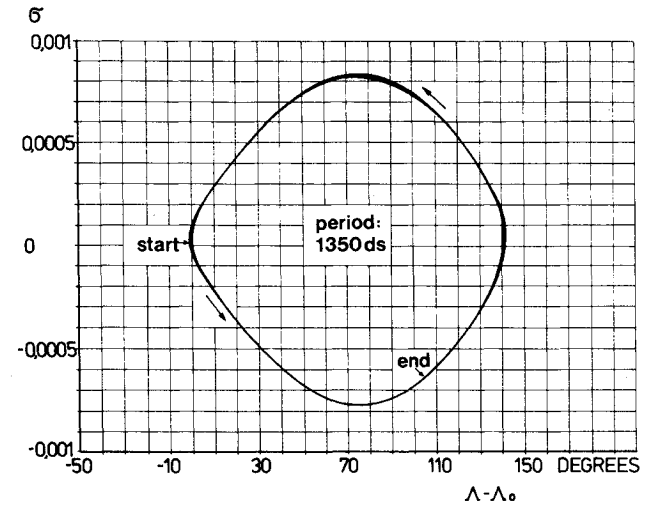

Fig. 4 Typical longitude drift vs semimajor axis deviation for satellite initially at 0 deg over 20 years.

The longitude drift coupled with variations in the semimajor axis is mainly caused by the J_{22} harmonic—the ellipticity of the Earth's equatorial cross section. Although the difference between the lengths of the equator's major and minor axes is only about 70 m, the perturbing force acts in a definite direction over a long term because of the close synchronism between the satellite's motion and the Earth's rotation. Therefore, a gradual buildup or decrease (depending on the location of the satellite) in energy and semimajor axis results. The satellite performs pendulum like oscillations (with periods longer than 820 days) around the nearest stable point, which lies on the extensions of the equator's minor axes at about 75° east and 105° west. Figure 4 shows the longitude drift under all perturbations over a period of 20 years for a satellite placed initially at 0 deg (Greenwich). After about 2 years, the satellite has drifted to 140° east, above Australia, where the drift starts reverting. It is important to recognize that the second and later trajectories almost exactly retrace the first one, so that the abandoned satellites will continue to move through the region occupied by the active satellites.

Probability Distribution of Active Satellites

In addition to longitudinal density variations due to preferred longitudinal locations, there exist characteristic radial and latitudinal density variations induced by the geometrical orbit properties between station-keeping maneuvers. It is assumed that the relative radial distance ρ and the latitude ϕ are given explicitly as functions of time by the first-order equations of the relative motion, while taking the mean elements e, i, and σ constant over one revolution.

Starting with the uniformly distributed random variable time and applying the standard transformations for functions of a random variable leads, after some approximations, to the radial-latitudinal density conditioned on the elements σ, e, and i (cf. Appendix):

$$f(\rho,\phi\,|\sigma,e,i) = \begin{cases} \dfrac{1}{\pi\sqrt{e^2-\rho^2}}\,\dfrac{1}{\pi\sqrt{i^2-\phi^2}}, & |\rho-\sigma|\le e, \quad |\phi|\le i \\ 0, & \text{otherwise} \end{cases} \tag{5}$$

This density displays the typical effects[5] of the oscillatory dynamics; namely, at some fixed instant in time, the satellite is more likely to be found near the extrema of the radial and latitudinal intervals than in the middle. The coupling of the radial and latitudinal motion has been removed by imposing rotational symmetry in longitude.

In the course of a station-keeping cycle, the mean elements on which the density mentioned above is conditioned are subjected to some typical dynamics of their own. For instance, between drift reversions the semimajor axis will uniformly increase or decrease with a rate depending on the reference longitude alone. The eccentricity vector will describe circular arcs under the effect of the solar radiation pressure, whereas the polar vector will mainly move parallel to the $i\sin\Omega$ axis (cf. Fig. 3). These dynamical effects, together with some natural assumptions on a minimum-effort station-keeping strategy, provide densities g_σ, g_e, and g_i for the elements. Thus, for a large population and for some fixed but unknown time instant, the conditioning on the instantaneous elements can be removed by averaging over the elements σ, e, and i:

$$f(\rho,\phi) = \int_\sigma \int_e \int_i f(\rho,\phi\,|\sigma,e,i)\,g_\sigma(\sigma)\,g_e(e)\,g_i(i)\,\mathrm{d}\sigma\,\mathrm{d}e\,\mathrm{d}i \tag{6}$$

This process finally leads to typical unconditioned densities of the form (cf. Appendix)

$$f(\rho,\phi) = \begin{cases} \dfrac{2\sqrt{e_m^2-\rho^2}}{\pi e_m^2}\,\dfrac{\ell n(i_m+\sqrt{i_m^2-\phi^2})}{\pi i_m}, & |\phi|\le i_m, \quad |\rho|\le e_m \\ 0, & \text{otherwise} \end{cases} \tag{7}$$

Different but similar results can be derived if other assumptions regarding the distributions of the elements are taken.

Results and Conclusions

Hazard Due to Abandoned Objects

On the basis of a sample set of orbit evolutions for some 30 abandoned objects with different characteristics, the probability of a collision with an active satellite was calculated. The dependence of the collisional rate on parameters of the abandoned objects such as initial data, initial longitude, and area/mass ratio and on parameters of the operational satellites such as width of the geostationary ring and distributions in the ring was evaluated. Other data variations were found to be less important. As a basis for comparisons with other results[6] the so-called Perek number N_P is introduced. This number is the *expected time in years to the first collision* calculated from the following stationary reference model:

1) There are 100 operational satellites in the ±0.1 deg geostationary ring.

2) There are 100 deactivated satellites all integrated from the same initial time and having uniformly distributed longitudes.

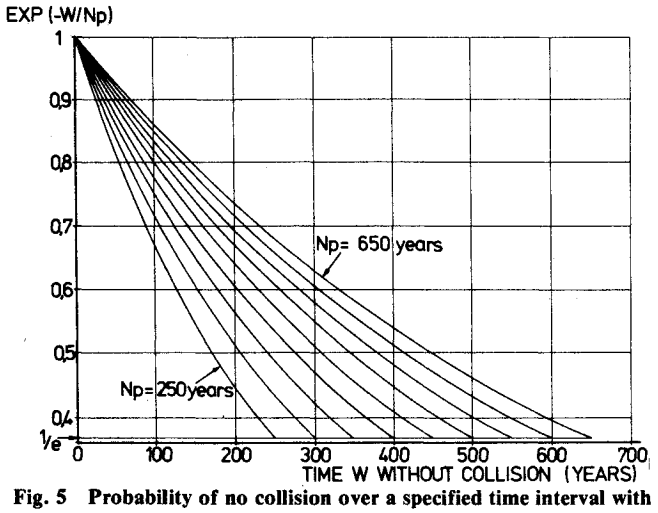

Fig. 5 Probability of no collision over a specified time interval with Perek number N_P as parameter.

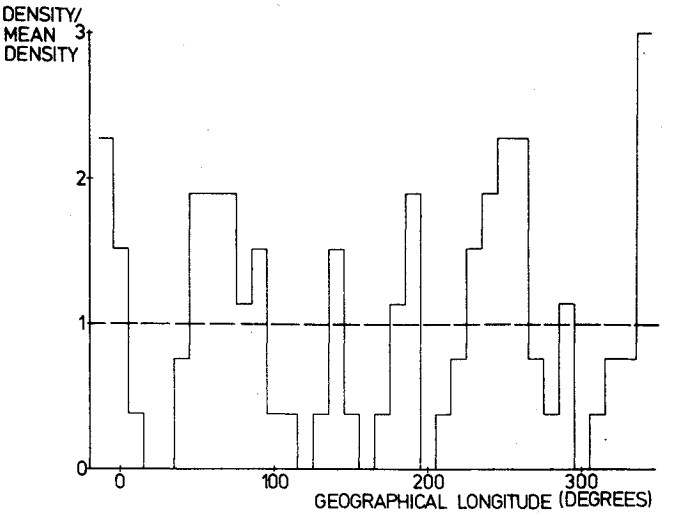

Fig. 7 Relative longitudinal density of active satellites.

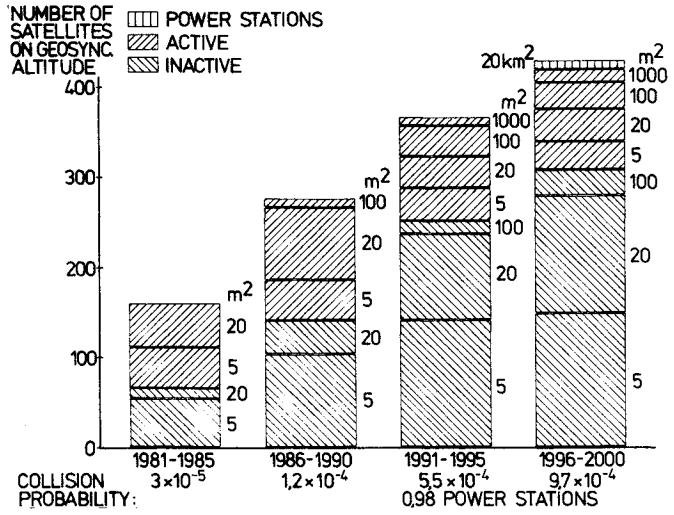

Fig. 6 Evolution of collision probability for extrapolated populations of satellites.

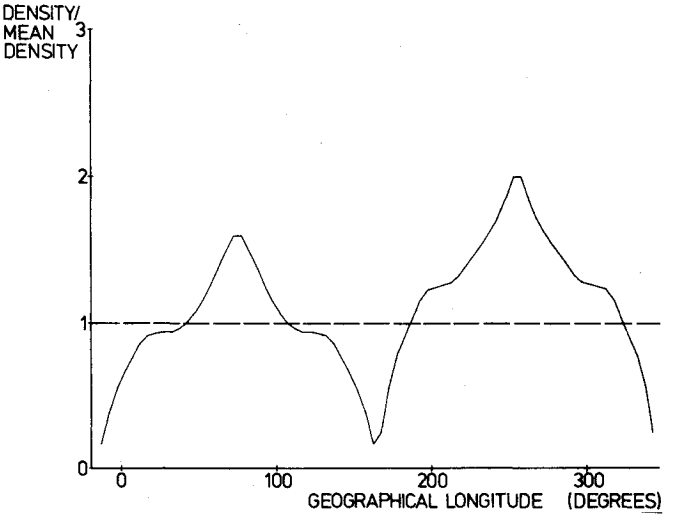

Fig. 8 Relative longitudinal density of deactivated satellites.

3) The collisional cross-sectional area is taken as $A_c = 800$ m^2, which corresponds to two satellites each of about 25-m radius.

4) The expected time until the first collision takes place is calculated from the collision probability obtained by considering a 20-year deterministic orbit evolution for the abandoned satellites.

This model may be considered to be somehow representative of the actual situation in the next few years. For different underlying assumptions, corresponding results can readily be derived from this basic number.

If the collision rate per year is denoted by λ, then the probability of at least one collision occurring in w years is given by

$$P(W \leq w) = 1 - e^{-\lambda w} \tag{8}$$

which is the (Poisson) distribution function of the time W without collisions. Thus the Perek number is $N_P = E(W) = 1/\lambda$. Plots of $\exp(-\lambda w)$ giving the probability of no collision over a certain time interval are given in Fig. 5 for a few typical Perek numbers. (The abscissa values of the curves at level $1/e$ correspond to their Perek numbers N_P.) It can be seen that a Perek number of 500 years, which approximately resembles the present-day situation, implies a 99% probability of no collision for only about 10 years.

For different area to mass ratios, initial dates, and longitudes, the Perek number varies betweeen 400 and 700 years. The corresponding collision rates λ_u, for one pair of objects per year and per unit collisional cross section of 1 km^2, vary between 0.17×10^{-4} and 0.31×10^{-4}. The width of the geostationary ring and the assumptions on the densities affect the probabilities in a consistent but not in a very essential manner.

Obviously, the probability of one very large satellite being hit by 100 small objects with 1 m^2 cross section each is greater than that of being struck by one object of 100 m^2 cross section. In the realistic case of inhomogeneous populations, the linear superpositions, corresponding to the previous assumptions, have to be replaced by a categorization according to the sizes of the satellites. The total collision rate per year can then be written as the sum

$$\lambda = \lambda_u \sum_{j=1}^{n} N_j \sum_{k=1}^{m} M_k (A_j^{1/2} + B_j^{1/2})^2 \tag{9}$$

where A_j, N_j, with $j = 1,\ldots,n$, and B_k, M_k, with $k = 1,\ldots,m$ are the cross sections and numbers per group of operational and deactivated satellites, respectively, and λ_u is the collision rate per unit area.

As an illustration, the populations and the corresponding satellite sizes were extrapolated for 5-year intervals until the year 2000. Figure 6 gives a visualization of the assumptions

made, as well as the resulting probabilities over the 5-year intervals. Although this extrapolation should not be interpreted as a very precise model of the real future evolution, it is obvious that the collisional risk will keep on growing and will become unacceptably large when solar-power satellites have to be taken into consideration.

In the results presented, the preference for certain longitudinal slots for communication and broadcast satellites has not been taken into account. Figure 7 shows the present longitudinal density relative to the mean density as collected from Morgan.[7] Assuming that the longitudinal preference remains the same during the coming decades, one arrives at the relative longitudinal density of deactivated satellites given in Fig. 8. It can be seen that satellites stationed at the stability points near 75° east and 105° west are subject to a collisional hazard which is about twice as large as the mean values quoted before.

Collisional Probability between Satellites Sharing the Same Longitudinal Slot

Due to the increasing demand for a few preferred longitudinal slots (Fig. 7), it is of interest to study the collision probability between operational satellites within the same 0.1 deg-longitudinal interval. On the basis of a few parametric runs evaluating the convolution integral introduced in Eq. (6), the following results were obtained:

1) The width of the station-keeping interval has little effect, which appears to be plausible in view of the fact that the relative velocity decreases when the density increases.

2) Other input variables such as the reference longitude have negligible influence as well.

The resulting collision rates turn out to be rather low. For instance, a pair of TV-Sats, each of 100 m^2 cross section, stationed in the same longitude slot have a collision probability of only 9×10^{-7}/yr. If, however, ten satellites rather than two were stationed on the same longitude location, the collisional hazard would grow by a binominal factor $\binom{10}{2}=45$. The time interval for which there is a 99% probability of no collision even then is still a few hundred years.

Conclusions and Recommendations

The major conclusions of the present study may be summarized as follows:

1) The dominant collisional hazard on the geostationary ring is due to an ever-increasing number of abandoned satellites, satellite components, and eventually secondary debris resulting from collisions.

2) All abandoned objects which are not actively removed from the geosynchronous altitude will permanently cross the ring for operational satellites, thus contaminating this unique and valuable resource for all foreseeable time.

3) Whereas, at present, the chance of a collision is rather small (about 6×10^{-6}/yr), it certainly will increase considerably over the next 20 years. With the appearance of solar-power satellites sometime in the future, it will become unacceptably high: Typically, collisions may then occur every 5 years.

4) The probability of collisions between several satellites stationed in the same 0.1 deg-longitude slot is relatively low due to the natural correlations in their motions.

5) The collision risk during station acquisition is negligible compared to the risks mentioned above.

An effective remedy for eliminating, or at least reducing, the collisional hazard in the future would be the removal of all geostationary satellites at deactivation to an altitude at least 100-150 km (depending on the area/mass ratio) higher. The cost in terms of incremental velocity would be no more than 3.65 m/s per 100-km altitude increase, which amounts to the fuel needed for about one month operational station-keeping. Numerical simulations over 200 years show that this increase in altitude would be sufficient to eliminate the risk of collision. Removal of obsolete satellites with different area to mass ratios to different altitudes would implicitly also reduce the secondary debris hazard.

Appendix: Derivation of Eqs. (5) and (7)

The uniformly distributed random variable time has the probability density

$$f_t(t)=2/T, \qquad 0\le t\le T/2 \tag{A1}$$

over one-half orbit (T is the period). The first-order relative motion in the local rotating frame can be written as

$$\begin{aligned}\lambda&=\lambda_d(\tau)+2e\sin\tau\\ \rho&=-e\cos\tau+\sigma(\tau)\\ \phi&=i\sin(\omega+\tau)\end{aligned} \tag{A2}$$

Here λ stands for the geographical longitude and $\tau=\omega_E t$; λ_d and σ designate drift terms. The derivatives with respect to τ can be expressed in the dependent variables λ,ρ,ϕ as follows

$$\begin{aligned}\lambda'&=-2\rho+\sigma/2\\ \rho'&=\pm[e^2-(\rho-\sigma)^2]^{1/2}\\ \phi'&=\pm(i^2-\phi^2)^{1/2}\end{aligned} \tag{A3}$$

Applying the standard transformation laws for the densities of functions of a random variable

$$f_\rho(\rho)=f_t(t(\rho))\left|\frac{d\rho}{dt}\right|^{-1}(\rho) \tag{A4}$$

and averaging over ω leads to Eq. (5)

In the derivation of Eq. (7), one typically assumes that the eccentricity vector

$$e=\begin{pmatrix} f\\ g\end{pmatrix}=\begin{pmatrix} e\cos(\omega+\Omega)\\ e\sin(\omega+\Omega)\end{pmatrix} \tag{A5}$$

is uniformly distributed on a circular disk

$$|e|\le e_m \tag{A6}$$

for some population of geostationary satellites. Then the joint density of f, g is

$$f_e(e)=\begin{cases}\dfrac{1}{\pi e_m^2}, & 0\le|e|\le e_m\\ 0, & \text{otherwise}\end{cases} \tag{A7}$$

Transformation to polar coordiantes (e,ψ) renders the joint density

$$g(e,\psi)=\begin{cases}\dfrac{e}{\pi e_m^2}, & 0\le|e|\le e_m\\ 0, & \text{otherwise}\end{cases} \tag{A8}$$

which, of course, turns out not to depend on the angular

variable ψ. The integration over e in Eq. (6) with $g_e(e) = 2\pi g(e,\psi)$ can now readily be executed. The consecutive averaging over i and σ is based on a similar approach with Eq. (7) as the result.

References

[1] Hechler, M., "The Probability of Collisions on the Geostationary Ring," European Space Operations Centre, MAO Working Paper No. 121, March 1980.

[2] Van der Ha, J.C., "Very Long-Term Orbit Evolution of a Geostationary Satellite," European Space Operations Centre, MAO Working Paper No. 122, March 1980.

[3] Chobotov, V.A., "Collision Hazard in Space," *Astronautics & Aeronautics,* Vol. 18, Sept. 1980, pp. 38-39.

[4] Kessler, D.J. and Cour Palais, B.G., "Collision Frequency of Artificial Satellites: The Creation of a Debris Belt," *Journal of Geophysical Research,* Vol. 83, June 1978, pp. 2637-2646.

[5] Dennis, N.G., "Probabilistic Theory and Statistical Distribution of Earth Satellites," *Journal of the British Interplanetary Society,* Vol. 25, May 1972, pp. 333-376.

[6] UN Committee on the Peaceful Uses of Outer Space, "Physical Nature and Technical Attributes of the Geostationary Orbit," Prepared by the UN Committee on the Peaceful Uses of Outer Space, A/AC. 105/203, Aug. 29, 1977; Addendum, Dec. 11, 1978.

[7] Morgan, W.L., "Geosynchronous Satellite Log," *Journal of the British Interplanetary Society,* Vol. 32, Oct. 1979, pp. 390-395.

From the AIAA Progress in Astronautics and Aeronautics Series

SPACE SYSTEMS AND THEIR INTERACTIONS WITH EARTH'S SPACE ENVIRONMENT—v. 71

Edited by Henry B. Garrett and Charles P. Pike, Air Force Geophysics Laboratory

This volume presents a wide-ranging scientific examination of the many aspects of the interaction between space systems and the space environment, a subject of growing importance in view of the ever more complicated missions to be performed in space and in view of the ever growing intricacy of spacecraft systems. Among the many fascinating topics are such matters as: the changes in the upper atmosphere, in the ionosphere, in the plasmasphere, and in the magnetosphere, due to vapor or gas releases from large space vehicles; electrical charging of the spacecraft by action of solar radiation and by interaction with the ionosphere, and the subsequent effects of such accumulation; the effects of microwave beams on the ionosphere, including not only radiative heating but also electric breakdown of the surrounding gas; the creation of ionosphere "holes" and wakes by rapidly moving spacecraft; the occurrence of arcs and the effects of such arcing in orbital spacecraft; the effects on space systems of the radiation environment, etc. Included are discussions of the details of the space environment itself, e.g., the characteristics of the upper atmosphere and of the outer atmosphere at great distances from the Earth; and the diverse physical radiations prevalent in outer space, especially in Earth's magnetosphere. A subject as diverse as this necessarily is an interdisciplinary one. It is therefore expected that this volume, based mainly on invited papers, will prove of value.

737 pp., 6 × 9, illus., $30.00 Mem., $55.00 List

TO ORDER WRITE: Publications Dept., AIAA, 1290 Avenue of the Americas, New York, N.Y. 10104